



## Digital camera calibration for cultural heritage documentation: the case study of a mass digitization project of religious monuments in Cyprus

Evagoras Evagorou, Christodoulos Mettas, Athos Agapiou, Kyriacos Themistocleous, Spyridon Papavasileiou & Diofantos Hadjimitsis

To cite this article: Evagoras Evagorou, Christodoulos Mettas, Athos Agapiou, Kyriacos Themistocleous, Spyridon Papavasileiou & Diofantos Hadjimitsis (2021) Digital camera calibration for cultural heritage documentation: the case study of a mass digitization project of religious monuments in Cyprus, *European Journal of Remote Sensing*, 54:sup1, 6-17, DOI: [10.1080/22797254.2020.1810131](https://doi.org/10.1080/22797254.2020.1810131)

To link to this article: <https://doi.org/10.1080/22797254.2020.1810131>



© 2020 The Author(s). Published by Informa UK Limited, trading as Taylor & Francis Group.



Published online: 02 Sep 2020.



Submit your article to this journal [↗](#)



Article views: 496



View related articles [↗](#)



View Crossmark data [↗](#)

## Digital camera calibration for cultural heritage documentation: the case study of a mass digitization project of religious monuments in Cyprus

Evagoras Evagorou<sup>a,b</sup>, Christodoulos Mettas<sup>a,b</sup>, Athos Agapiou<sup>a,b</sup>, Kyriacos Themistocleous<sup>a,b</sup>, Spyridon Papavasileiou<sup>c</sup> and Diofantos Hadjimitsis<sup>a,b</sup>

<sup>a</sup>Department of Civil Engineering and Geomatics, Faculty of Engineering and Technology, Cyprus University of Technology, Lemesos, Cyprus; <sup>b</sup>Eratosthenes Centre of Excellence, Lemesos, Cyprus; <sup>c</sup>Holy Bishopric of Limassol, Lemesos, Cyprus

### ABSTRACT

The paper summarizes the methodology followed, to evaluate the accuracy of different digitization methods of ecclesiastical monuments in 3D computer vision form and stresses the importance of photographic equipment calibration. In this study, a set of images were taken using the CANON EOS M5 digital camera, while the internal calibration parameters – horizontal and vertical focal length ( $f_x$ ,  $f_y$ ), principal point coordinates ( $x_0$ ,  $y_0$ ), radial distortion coefficients ( $K_1$ ,  $K_2$ ,  $K_3$ ), tangential distortion coefficients ( $P_1$ ,  $P_2$ ) and the affinity and the shear terms ( $b_1$ ,  $b_2$ ) were estimated. These parameters were calculated using different software applications and then analyzed. For the calibration procedure, 3D texture models were built with the Agisoft commercial software based on: (a) the aforementioned calibration parameters and (b) the self-calibration process. The overall accuracy (Root Mean Square – RMS) between these models, by comparing known geo-referenced ground-control-points (GCP) is presented through the Cloud Compare software. The results indicate that the internal calibration parameters of the digital camera used for documentation purposes are essential and should be systematically implemented for documentation purposes.

### ARTICLE HISTORY

Received 23 November 2019  
Revised 4 August 2020  
Accepted 10 August 2020

### KEYWORDS

Camera calibration; cultural heritage; self-calibration; pre-calibration; lens distortion

### Introduction

Visualization of buildings and infrastructure in 3D form has been widely applied mainly through photogrammetric procedures. In addition, the broad spectrum of close-range photogrammetric applications has supported the growing trend of 3D documentation of Cultural Heritage monuments and sites (Pierdicca et al., 2016). The documentation provides vital information regarding the restoration of ancient monuments and the potential re-use of documentation results (Remondino & Rizzi, 2010). 3D scanning and photogrammetry technologies are particularly valuable for fast spatial data collection from existing buildings including intervention when conditions are dangerous (Themistocleous et al., 2019). The 3D data obtained from 3D scanning and photogrammetry technologies are fast and low-cost especially when compared to traditional documentation methods. 3D modeling through terrestrial laser scanners (TLS) and close-range photogrammetry are widely used in various sectors, including Historic Building Information Modelling (HBIM) (Themistocleous et al., 2018).

The project “Digital Aposphragisma (Imprint) of Hagionymous Islands” aims to implement traditional topographic and photogrammetric methods for documentation and management purposes, as well as the promotion of ecclesiastical cultural heritage. The

project proposes the development of digital database infrastructure for storing and managing documentation data and metadata, as well as other enrichment digital tools for providing comprehensive digital and documentation cultural evidence. The current research, regarding 3D documentation, focuses mainly on single standing monuments and sites. In contrast, the “Digital Aposphragisma (Imprint) of Hagionymous Islands” project aims to develop a robust methodology for mass digitization, that requires both fast and accurate documentation and processing. For this reason, the digital documentation record of the ecclesiastical cultural heritage of the island of Cyprus includes a variety of documentation procedures such as close-range photographs, stereo-pairs, images from Unmanned Aerial Vehicles (UAVs), point clouds from terrestrial laser scanners (TLS), points from Total Stations, etc., both internally and externally of building facades and relics of selected monuments.

There is a great deal of research regarding the various methodologies for developing 3D digitization models. De Reu et al. (2013) proposed a 3D cost-effective registration and extraction of 3D point clouds from ordinary 2D images using the structure – from – motion (SfM) method and dense image stereo-matching of archaeological heritage sites. In both the 2D and

3D forms, the results have a high accuracy, which can be integrated with the archaeological excavation plan. Several studies indicate how cultural heritage sites can be monitored using 3D scanning, photogrammetry and close-range cameras (Abed et al., 2019; Tucci et al., 2017). Several studies have also incorporated the use of close-range UAVs for 3D documentation (Aicardi et al., 2018; Murtiyoso et al., 2017; Themistocleous, 2017).

A vital step, in developing 3D computer vision for the extraction of reliable metric information from images, is the interior orientation of the camera, known as “camera calibration”. Camera calibration must be conducted for a precise 3D computer vision model and should be performed on any camera for the correction of distortion and intrinsic parameters of the camera lens, in order to extract more accurate results. The camera calibration method can be conducted either before image-acquisition (photogrammetric calibration procedure) or during the modeling process, which comprises the extraction of the 3D model data (self-calibration procedure).

In the self-calibration method, where no calibration object is used, since the calibration is performed by moving a camera in a static scene, the camera displacement of the images is used to estimate the camera’s internal parameters (Faugeras et al., 1992). Self-calibration has been widely accepted as an efficient technique in close-range photogrammetry by using additional parameters. Photogrammetric self-calibration is a function approximation based on the Weierstrass theorem. According to Fraser (1997) the 10-parameter self-calibration model used for close-range digital cameras has yielded object-space triangulation precision well beyond 1:100,000. Research on the Brown self-calibration model examines the calibration parameters of the zoom effects proposing image coordinate correction models for interior orientation and lens distortion (Fraser & Al-Ajlouni, 2006; Schad & Engbert, 2012). Tang and Fritsch (2013) stated that the compensation of distortion can be achieved based on additional parameters (APs) through orthogonal functions. The polynomial additional parameters are revaluated and the renamed Legendre self-calibration APs (Tang et al., 2012). Pollefeys et al. (1999) found that it is possible to use only the most general constraint in the self-calibration method (i.e. that image rows and columns are orthogonal); however, better results can be obtained if more constraints are available. Many flexible calibration algorithms (Sturm & Maybank, 1999; Zhang, 2000; Zhang et al., 2011) were designed to calibrate lens from correspondences on a planar object captured from a few different views whereas the radial lens distortions can be estimated and consisting of a closed-form solution, followed by a nonlinear refinement based on maximum likelihood criterion. In

addition, a method proposed calibrating several cameras in a short period of time with no manual intervention (Fiala & Shu, 2008).

The self-calibration and pre-calibration method of a low-cost camera with lenses of different focal lengths has been implemented in many studies (Brutto & Dardanelli, 2017; Zacharek et al., 2017) in order to estimate the internal orientation of the camera. The calibration was tested using different software packages, concluding that the most accurate deployed software program was Image Master (Fryskowska et al., 2016). Research on archaeological monuments in Nepal evaluated the feasibility of low-cost photogrammetric modeling cultural heritage sites. Two 3D point clouds were created: (a) using photogrammetry with self-calibration technique, (b) using a high precision laser scanner. The extracted results show that the accuracy of the two compared point clouds varied from 2 to 5 cm (Dhonju et al., 2017).

Even though close-range photogrammetry was widely and systematically used in the past to document cultural heritage monuments and sites, and also was compared with other documentation techniques such as terrestrial laser scanners and topographic measurements, a detailed study regarding the calibration process of relatively low-cost photographic equipment (known as internal orientation in photogrammetry) was required, as part of an ambitious research project aiming to produce mass-documentation datasets for Cyprus’s ecclesiastical heritage. The analysis of these calibration methods was performed through various software and the extracted 3D models are represented in this study. Also, an evaluation for each 3D model was performed using control points and point clouds through terrestrial laser scanners. The workflow aims to evaluate the various calibration strategies for each camera indicating the expected accuracy in 3D-modelling.

## Study area

Churches in the Limassol district in Cyprus were mapped for the purpose of the project (see Figure 1). The data collection performed for the church of Panagias Harmatziotissas, outside of the modern village of Kapileio are presented in this study. The church was constructed during the fifteenth century and is now in ruins. Part of the church collapsed and only the walls are visible. This type of church, is a small size basilica, with an ordinary oblong external shape with a semi-cylindrical apse at the east end, while the internal recesses indicate that it was barrel-vaulted edifice with two stiffening arches (sfendonia) coming across latitudinally reinforcing the vault (Holy Metropolis of Limassol, 2016). The geographic coordinates of the site are 34°49'1.2"N, 32°57'57.6"E, as can be seen in Figure 1.

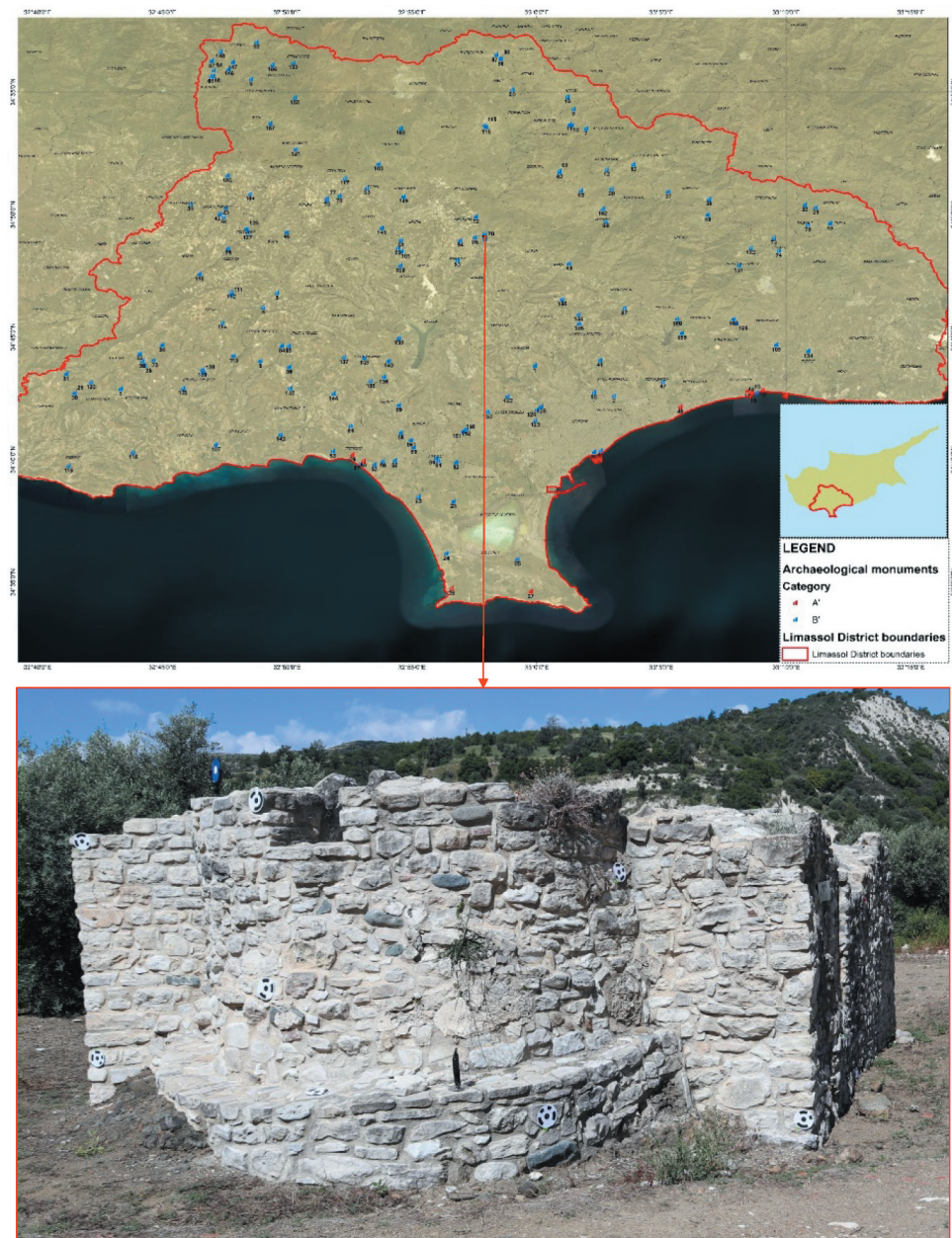


**Figure 1.** Archaeological churches in the province of Limassol, Cyprus – Location of the church of Panagias Harmatziotissas.

## Methodology

Photogrammetry was used in fields such as geology, architecture, archaeology, etc. The main advantage of photogrammetry is the fast acquisition of data at a low operating cost. The terrestrial photogrammetry used in several studies (Koutsoudis et al., 2014; Strecha et al., 2014) is based on non-metric cameras. Consequently, in recent years, the use of close-range cameras is widespread, mainly, using low-cost cameras and software applications.

This section describes the workflow used for calibration of the camera, data collection and analysis of data (Figure 2). These sections describe methodologies, techniques and equipment that were used to collect and process the data. The study focuses on the calibration methodologies comparing the results

with self-calibration and pre-calibration of the cameras for various focal lengths. The validation of these results was carried out using laser scanner data showing the deviations and errors for each method used.

The four major steps for the generation of the dense point cloud using the self-calibration are: (a) automatic detection of the targets and assignment of the coordinates of the measured targets, which can lead to improving the photo-alignment procedure, defining the local coordinate system and scaling the model, (b) alignment of the images where the accuracy was set to high in order to use full image resolution and (c) generation of the dense cloud. The final step was performed at five different levels. For the study area, medium resolution level was deemed acceptable, generating 45 million points.

Using the pre-calibration option, a fourth step was added to the workflow. Before the alignment, the pre-

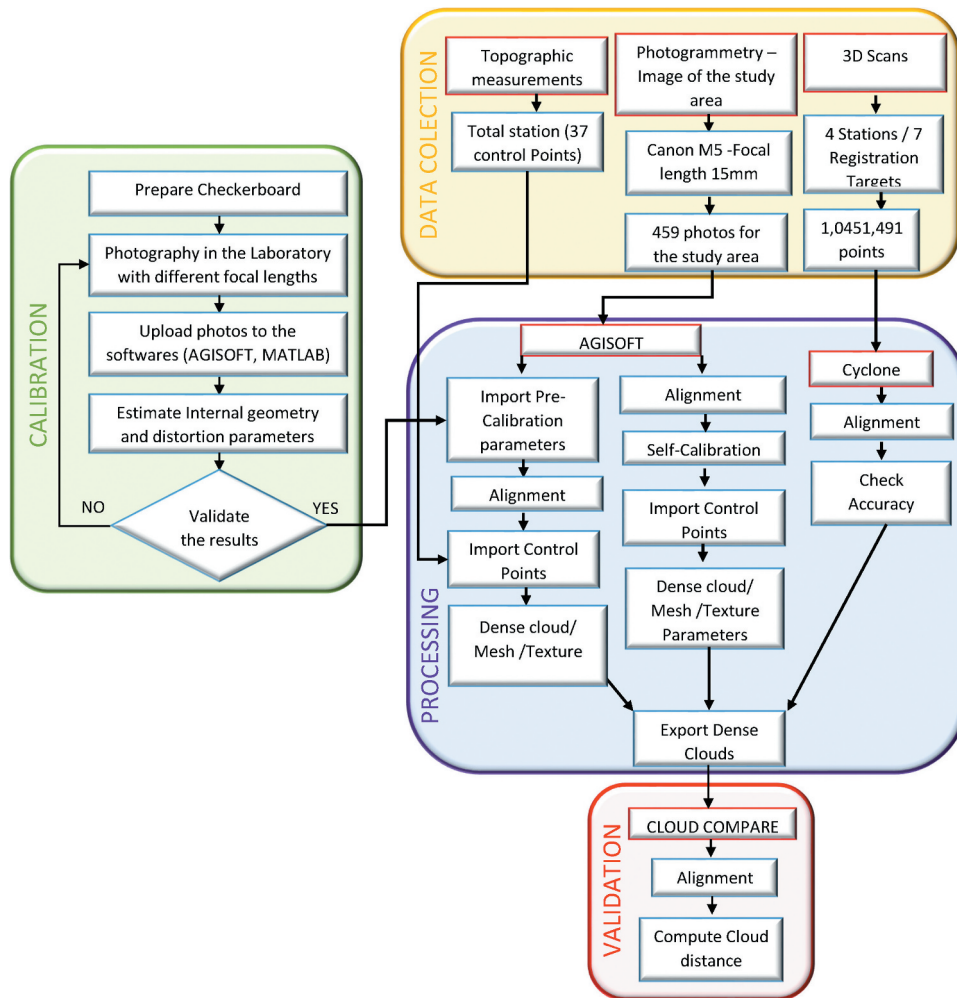


Figure 2. Workflow for data collection and processing.

calibration parameters were saved to the software. The next steps consider the extraction of two different point clouds using the MATLAB and Agisoft pre-calibration parameters. The final step (d) is the comparison and evaluation of the final results.

### Camera calibration

A very significant step of 3D modeling is the camera calibration, as the precise determination of the internal geometry parameters can address any distortion. The camera calibration is used to determine precisely, the parameters of the internal geometry of the camera that should be repeated at regular intervals in the laboratory. The focal length used during the photographic shots is constant for each shot and can be accurately calculated using several control points. The determination of the internal geometry of the camera can be achieved either based on the self-calibration or the pre-calibration strategy.


The main purpose of this study is to implement both techniques on the same ecclesiastical monument. The CANON EOS M5 camera was used with a focal length of 15 mm for the pre-calibration of the camera.

The main specifications of the camera are stated in Figure 3.

The self-calibration method is achieved by using the camera displacement of the images in order to estimate the camera's internal parameters. Self-calibration is performed during the processing of the images in order to calculate the parameters of the camera's internal geometry. For the self-calibration method, the option of the calibration of the lens was used in the Agisoft software during the 3D modeling of the church. In the case of the pre-calibration method, the work was processed using Agisoft and MATLAB software to estimate the internal parameters of the camera.

### Pre-calibration

Pre-calibration of the camera was made through the module of Agisoft Lens in which the screen of a personal computer was used as a calibration target. To take a photograph of the target, the Agisoft instructions were followed and the set of images was uploaded to the software in order to estimate the calibration parameters of the camera. Furthermore,

	<b>Name</b>	<b>Canon M5</b>
	Effective Pixels	24.2 MP
	Resolution	6000 x 4000
	Pixel size (mm)	0.0037211 x 0.0037211
	Focal Length	F = 15mm – 45 mm
Sensor Size	22.3 x 14.9mm	

**Figure 3.** Specifications of camera.

the MATLAB Camera Calibrator was used in order to determine the calibration parameters of the camera. This camera model is inspired by the model proposed by Heikkila and Silven (1997) with further distortion correction.

The calibration algorithm of the referred software uses the camera model which includes the pinhole camera model and lens distortion. The pinhole camera models applied Equation 1:

$$\begin{pmatrix} x \\ y \\ z \end{pmatrix} = K * \begin{pmatrix} X \\ Y \\ Z \end{pmatrix} \quad (1)$$

where  $X, Y, Z$  are the coordinates in a reference system,  $x, y, z$  represents the image-coordinates,  $K$  is the rotation matrix defining the camera orientation that can be found through Equation 2:

$$K = \begin{pmatrix} f_x & 0 & 0 \\ s & f_y & 0 \\ c_x & c_y & 1 \end{pmatrix} \quad (2)$$

where  $f_x, f_y$  define the focal length in pixels,  $c_x, c_y$  are the principal points coordinates and  $s$  is the skew coefficient. By combining the above equations, Equation 3 is obtained:

$$\begin{pmatrix} x \\ y \\ z \end{pmatrix} = \begin{pmatrix} f_x & 0 & 0 \\ s & f_y & 0 \\ c_x & c_y & 1 \end{pmatrix} * \begin{pmatrix} X \\ Y \\ Z \end{pmatrix} \quad (3)$$

The above calibration corrects the lens's distortion, scales and geo-references the final results in a world unit, thereby indicating the location of the camera in

the scene. The equation of distortion depends on the angle between the lens and the main radius and on the radial distance, as can be seen in Equation 4:

$$\Delta r = r - f \cdot \tan \theta \quad (4)$$

where  $\Delta r$  is the radial distortion,  $r$  is the radial distance ( $r^2 = (x_0 - X')^2 + (y_0 - Y')^2$ ),  $f$  is the focal length and  $\theta$  is the angle of the scene. The equations of the radial distortion can be represented using a polynomial with the radial distance (Equation 5). Equations 6 and 7 are applied to estimate the distorted coordinates using the distortion parameters and can be seen below:

$$\Delta r = k_1 r^2 + k_2 r^4 + k_3 r^6 \dots \quad (5)$$

$$\left. \begin{aligned} X' &= \Delta x_{radial} + \Delta x_{tangential} \\ Y' &= \Delta y_{radial} + \Delta y_{tangential} \end{aligned} \right\} \quad (6)$$

$$\left. \begin{aligned} X' &= x(k_1 r^2 + k_2 r^4 + k_3 r^6) + 2p_1 xy + p_2(r^2 + 2x^2) \\ Y' &= y(k_1 r^2 + k_2 r^4 + k_3 r^6) + p_1(r^2 + 2y^2) + 2p_2 xy \end{aligned} \right\} \quad (7)$$

where  $X', Y'$  are distorted coordinates,  $k_1, k_2, k_3$  are the radial distortion coefficients and the  $p_1, p_2, p_3$  are the tangential distortion coefficients.

Generally, the pinhole camera model for lens calibration and Brown's distortion model for distortions are used by Agisoft and MATLAB. Using Agisoft software, photos from the checkerboard were taken from the computer's screen while for the photos that have been used in the MATLAB, a checkerboard was printed on a hard flat surface (Figure 4). The printed checkerboard had a dimension  $594 \times 841$  mm with the

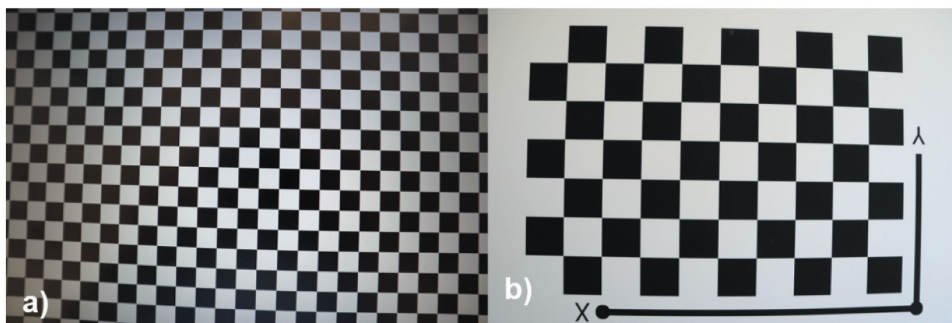


**Figure 4.** a) Agisoft checkerboard, b) MATLAB checkerboard (size of checkerboard square: 63.44 mm x 63.44 mm).

size of checkerboard square to be 63.44 mm x 63.44 mm. Ensuing photo shooting of the pattern and from the computer's screen in different views was performed and 45 images were uploaded in Agisoft software and 25 in MATLAB to calibrate the camera. Subsequently, evaluation and adjusting of parameters were achieved in order to improve the calibration accuracy. The mean projection error of the calibration using the MATLAB toolbox is smaller than 0.5 pixel.

### Data acquisition

The data collection was carried out on May 8<sup>th</sup>, 2019. The geodetic instruments used to collect in-situ data were the Leica GNSS receiver GS15 and Leica total station TCR 1203 +. Thirty-seven (37) automatic recognition targets (blue flags, Figure 5), with a 12-bit pattern of the Agisoft software, were placed in the archaeological monument and scanned with the aforementioned geodetic instruments (green signs, Figure 5). Also, laser scanner imprint was essential to cover as many monument's surface as possible to validate the results. The 3D scanning was conducted using the Leica C10 laser scanner and was set at medium resolution (1 cm grid at a distance of 10 m). Using 4 scans with a range distance between the scan-station and the monument of 2–15 m, over 80% of the surface was covered. An average distance between two consecutive points of the point cloud was estimated as 1.64 cm. Seven targets were evenly placed in the digitized environment for the registration. In total, the four scan stations (orange signs) that were registered with seven targets (red flags) can be seen on the sketch in Figure 5. These seven targets were (Figure 5(b)) Laser Scanner C10 targets measured with TCR 1203+ for georeferencing and alignment registering of the four-point clouds. Complete digitization was not achieved using the laser scanner because the monument height

ranges from 0.6 m to 2.5 m. A complete digitization of the monument would require at least one station stop, using a scaffolding construction to scan the high points of the monument.

Proper camera settings, as well as data collection planning, are crucial steps in data acquisition for photogrammetry. It is important to adjust the camera settings to maintain throughout the course of photography (Marčič, 2014). In this case study, the monument was photographed with the camera CANON EOS M5. The camera was adjusted so that the photos were not dark, blurry and unfocused. The camera's settings for this study area were set to a focal length of 15 mm, ISO of 100, F-Stop (Aperture) of F/8 and the exposure time was set to 1/400 sec. SfM was used as it functions under the same basic tenets as stereoscopic photogrammetry and can be resolved from a series of overlapping, offset images (Roncella et al., 2011; Schönberger & Frahm, 2020; Westoby et al., 2012). Structure-from-Motion (SfM) strategy functions under the same basic tenets as stereoscopic photogrammetry and can be resolved from a series of overlapping, offset images. Two circles of photo shooting completed in 5.5 and 2-m average distance from the monument, with the overlapping of the consecutive photos exceeds 70%. A two-meter monopod was used during the photography that assisted steady shooting. The Canon Camera Connect mobile application for the remote shooting was used to take over 450 images over 2 m from ground level.

### Data processing

The primary output of the processing of the above data is the precise creation of the point clouds, which represent the shape and size of the structure. Mesh and structural digital elevation models, which are used to preserve cultural heritage, can be extracted from the raw point clouds.



Figure 5. a) Agisoft Target points, b) Laser Scanner C10 targets and c) Surveying sketch.

After the implementation of data acquisition, the analysis and extraction of the cloud points were followed.

Cyclone, Agisoft and CloudCompare software were used for the output of dense clouds and the estimation of the distance errors. Dense clouds of the laser scanner data were processed using the Cyclone software, which was able to use the measured targets to achieve the alignment of the four laser scanner point clouds. Following, the production of dense clouds using the self-calibration and pre-calibration methods was conducted.

The following steps were followed in order to create the 3D model using Agisoft. The first step was to upload all the images into the software and proceed to automatic detection of targets, thereby keeping only 25 GP's targets, in order to improve the photo-alignment process. Subsequently, the coordinates of 25 GCPs were imported in order to define the local coordinate system and the scale of the 3D model. Following, the processed images were masked to remove any object not to be considered on the alignment, such as sky, people, etc. The next processing step is the self-calibration or pre-calibration to proceed to the alignment. The images were aligned using the highest accuracy option and setting up the key points to 50,000 and to 5000 for the tie points. The medium quality was chosen to build the dense cloud using the moderate option for the depth filtering. Noise elimination was implemented on the dense cloud, and the dense cloud was exported as a .obj extension. For the pre-calibration models, the only difference in the model's extraction method was the import of calibration parameters that were extracted from the above methodology.

## Results

### Calibration

In terms of the calibration procedure, the error values should not exceed the value of one pixel. Images with errors that exceed the value of one pixel were removed from the process. In the case where the numbers of the photos were less than 10, the calibration had to be reinitiated. The final results of the pre-calibration of CANON EOS M5 after the validation of the camera calibration can be found in Table 1. The pre-calibration data from the Agisoft software lens vary from the other two mainly due to the use of a different grid and photo-shooting attributes performed for calibration. The focal length was set to 15 mm for the study area and therefore only these values were used for processing of the pre-calibration parameters.

### Dense cloud from 3D scanning

The registration of the four-measured scans was completed by importing data of the four-point clouds and the seven measured targets through the Cyclone

**Table 1.** Results of the camera calibration.

	S-C: Agisoft	P-C: Agisoft	P-C: MATLAB
No	458	45	10
F	15	15	15
f	4145.25	4161.198	4189.078
cx	0.846	-23.738	-0.449
cy	-14.32	14.793	12.663
b1	0	-1.867	-8.044
b2	0	2.590	-0.120
k1	-0.134	-0.109	-0.137
k2	0.102	0.074	0.117
k3	-0.022	0.002	-0.003
p1	-0.001	-0.002	-0.002
p2	-0.001	-0.002	-0.002

S-C: self-calibration, P-C: pre-calibration, No: Number of photos, F: focal length in mm, f: focal length measured in pixels, b1 = fx - fy, b2 = skew, cx: principal point x-coordinates, cy: principal point y-coordinates, k1& k2: radial distortion coefficients, p1 & p2: tangential distortion coefficients.

software. The registration and alignment of the laser scanner data provided an accuracy of less than 5 mm. Subsequently, the focused area was defined by removing unnecessary information, and denoising was applied to the point cloud. This point cloud of laser scanner was used to validate the cloud points that were extracted by different methods of calibration (pre-calibration, self-calibration). The alignment errors produced by using the measured targets range between 0.002 m to 0.005 m. Figure 6 features the aligned dense cloud of the laser scanner that was processed through the Cyclone software. The generated point cloud was used to study the geometrical errors of the Agisoft point clouds align.

### Dense cloud using photogrammetry

A total of 459 images and 37 measured targets were uploaded to the Agisoft software in order to advance with the dense cloud creation. The 25 targets were used as Ground Control Points (GCPs) and the remaining 12 targets as Check Points (CPs). GCPs were used during alignment/georeferencing and CPs were used to calculate errors. Point separation was done because the point determination must be independent during the alignment process to achieve the absolute precision. Nevertheless, in the process of alignment, an estimated error of 25 points indicated the internal accuracy during the calculation. Following the alignment procedure using the control points, the distance errors were given to an overall report of the processing. These errors are provided in Table 2, indicating the mean errors between the targets and the surveyed points on the field. The observed fluctuations of the errors were related to the different values of calibration parameters. The estimated range of the GCP's errors (1.54–1.56 cm) was mainly due to the total station accuracy and the leveling of instrument/prism during the surveying.

As seen in Table 2, the lowest RMSE on the GCPs and CPs was generated in the dense cloud with pre-calibration using the Agisoft software and the higher errors were observed during self-calibration.



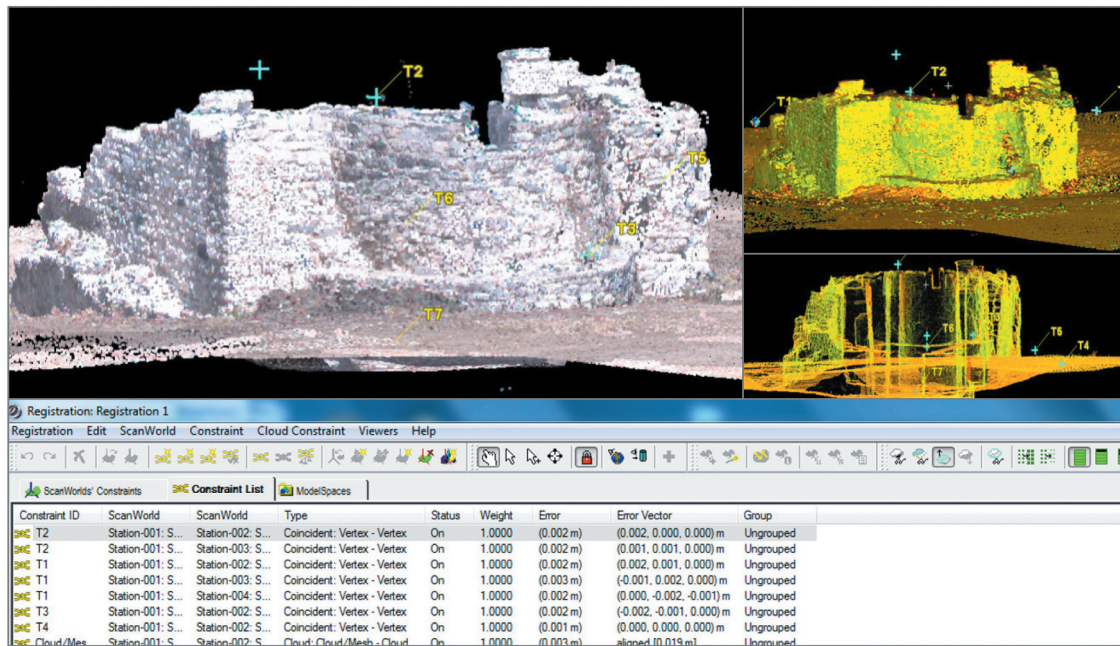


Figure 6. Dense Cloud from Laser scanner.

Table 2. Control point root mean square error (RMSE).

Type of calibration	Software	No of GCPs	No of CPs	X error (cm)	Y error (cm)	Z error (cm)	XY error (cm)	Total (cm)
Self-calibration	Agisoft	25	-	0.45	0.66	1.34	0.80	1.56
		-	12	0.47	0.54	1.25	0.72	1.45
Pre-calibration	Agisoft	25	-	0.45	0.69	1.31	0.82	1.55
		-	12	0.44	0.55	1.20	0.70	1.39
	MATLAB	25	-	0.46	0.69	1.31	0.83	1.55
		-	12	0.47	0.54	1.25	0.71	1.44

The dense clouds for the study area were extracted using the methodology of this study. Overall, 45 million points for each point cloud were generated and the finalized results were used for comparison and evaluation. One of the outcomes of the Agisoft report is a graph showing the camera locations and the image overlapping. As can be seen in Figure 7(a), the overlapping was achieved by more than nine photos, which is a satisfactory number for the generation of dense clouds. Also, the Image residuals were retrieved for CANON EOS M5, with the focal length set to 15 mm, in which it shows the average vector of the reprojection error for the pixels in the corresponding cells. Image Residuals (Figure 7(b–e)) feature the average vector of the reprojection error for the pixels in the corresponding cells. Figure (b) shows the model distortion that the Agisoft software uses for self-calibration. As can be seen in Figure 7 (c–d), the distortion of the lens of the pre-calibration has similar results and more distortions were observed at the edge of the pixels.

### Comparison and evaluation

The comparisons and evaluations of the outputs of the process were made according to the results of the dense cloud produced by the high precision laser

scanner (Leica C10), while the errors of the dense cloud were considered as zero. The CloudCompare processing software was used to perform a direct comparison between the dense clouds produced using the different procedures and software. All the point clouds were in scale, but the dense cloud of the laser scanner was not georeferenced. Following the command of the “Align by picking points”, the georeferenced point cloud was achieved using the laser scanner’s seven measured targets. A segmentation was applied in all dense clouds using the same polygon in order to compare the same area of the point clouds. Afterward, the mathematical model quadratic was used because it is more precise; however, they require more time to calculate. The radius of a spherical neighborhood of 15 cm was chosen in order to compare more points between the point clouds. The final results of the statistical errors of each dense cloud can be seen in Figure 8.

The results show the error distributions of the archaeological monument with near-precision between the dense clouds. Figure 8(a–d) shows the distribution of errors. The flat surfaces of the monument were accurate, while principal errors occurred on the ground surface. The results using the pre-

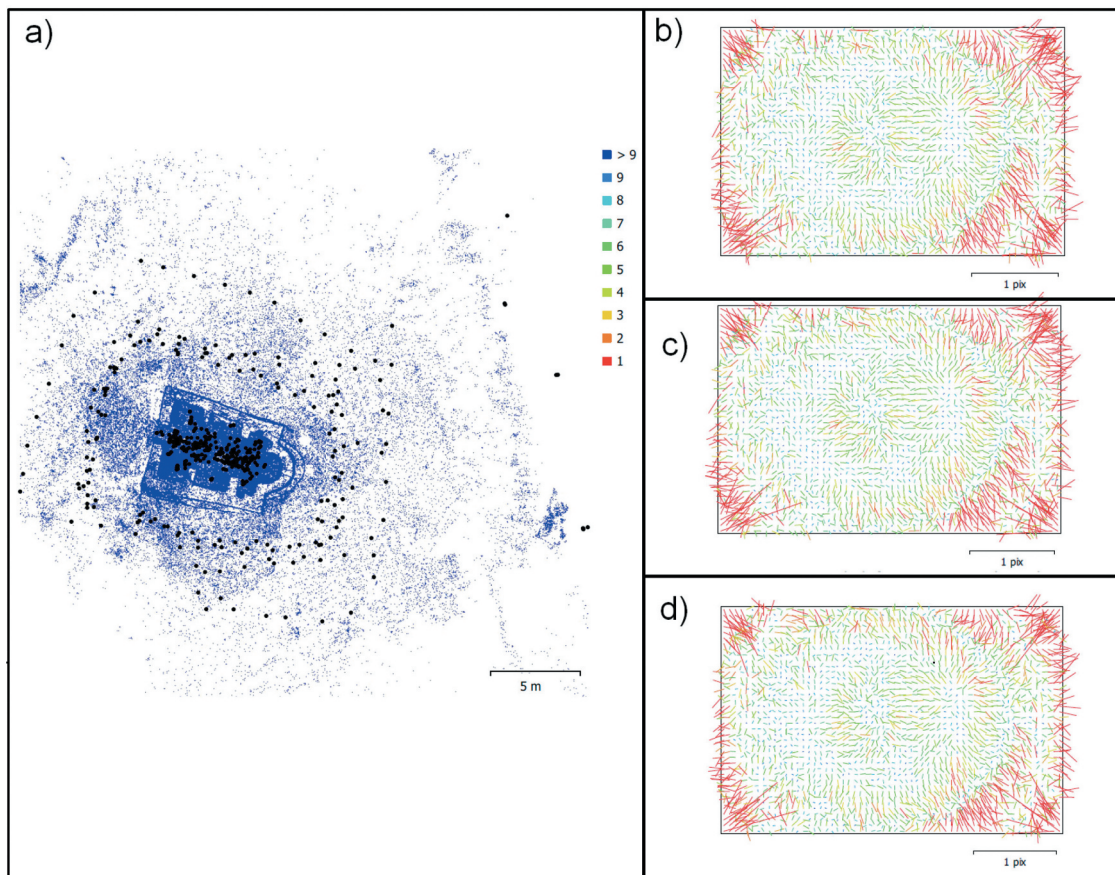


**Figure 7.** a) Overlapped images, b) Self-Calibration distortions using Agisoft, c) Pre-calibration distortions using Agisoft and d) Pre-Calibration distortions using MATLAB.

calibration strategy have a better accuracy compared to those with self-calibration. In particular, the histograms from Figure 8(i–iv) show that the results of pre-calibration (MATLAB) seem to have the best results with the RMS error 7.21 mm and standard deviation  $\pm 5.35$  mm. The results of pre-calibration with the Agisoft software (RMS 7.42 mm and standard deviation  $\pm 5.44$  mm) and self-calibration errors with the RMS being 7.43 mm and standard deviation  $\pm 5.37$  mm. In comparing the results between self-calibration and pre-calibration, more accurate results were observed with pre-calibration by 0.13% (Agisoft) and 2.96% (MATLAB). The comparison results can be found in Table 3.

### Discussion – conclusions

Three-dimensional (3D) visualization of cultural heritage monuments using low-cost cameras has been widely studied in the past (Bolognesi et al., 2015; Caradonna et al., 2018; Verhoeven, 2011). Several studies used either the self-calibration or pre-calibration and calculated the precision. This paper referred to the methods of calibration and data acquisition to achieve the comparison of the results of the archaeological monument of Panagias Harmatziotissas in the village of Kapileio, in Limassol, Cyprus. Data

acquisition was achieved with close-range cameras (CANON EOS M5) as well as topographic equipment: Total Station and Laser scanner. The calibration results were used in the monument mapping for the extraction of point clouds. The fact that the image-based results are comparable with the laser scanner point clouds assisted in the evaluation of the final results.

Using the above-described methodology, the results were used as part of a European-funded project to extract 3D models of archaeological monuments in Limassol area, Cyprus. The evaluation of the results showed a strong correlation with those of the laser scanner with RMS errors ranging at 7 mm. The comparison revealed that pre-calibration models generate 0.13–2.96% more accurate results than those with self-calibration.

In conclusion, the study indicates that the pre-calibration of all the cameras or different focal lengths of the same camera to be used for the three-dimensional vision of the archaeological monuments should be calibrated using the module Agisoft’s “Calibrate lens” for more accurate results. As Agisoft software is used for generating the 3D models, an additional benefit of the software is the calculation of the additional Radial and tangential distortion coefficients that cannot be provided by MATLAB.

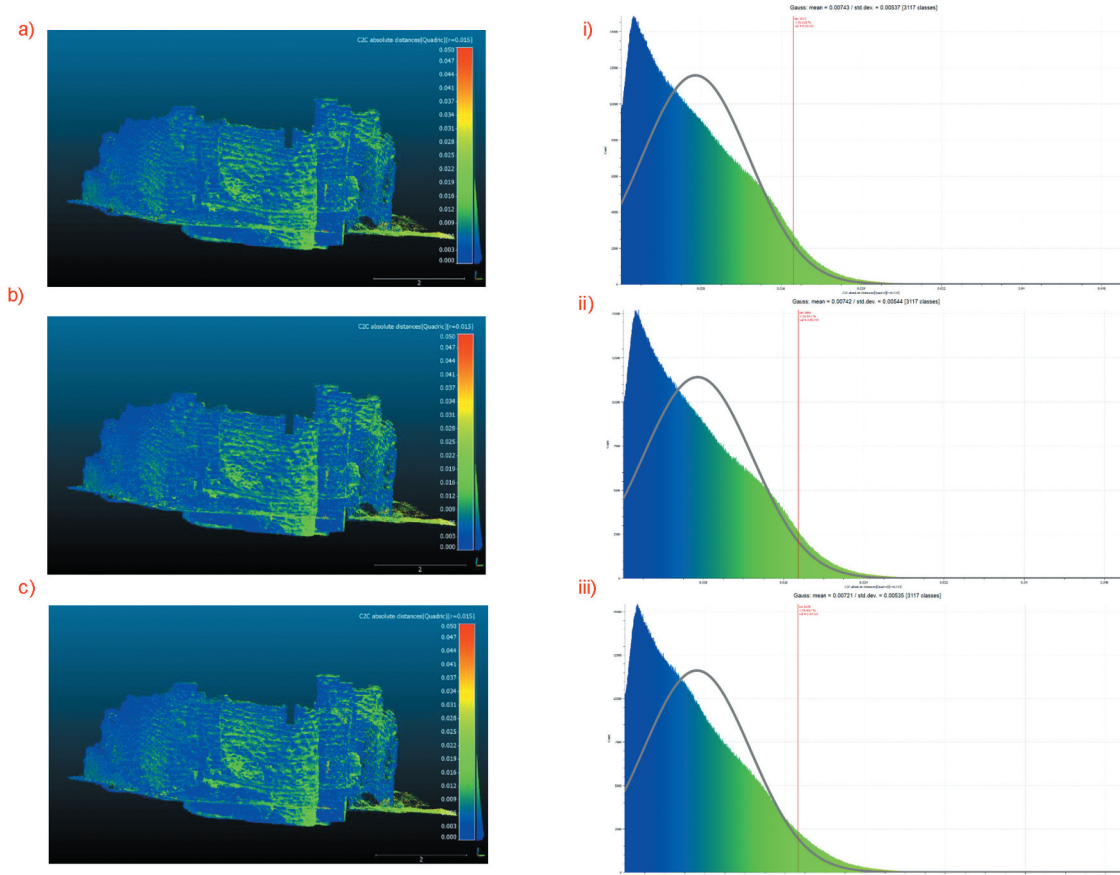


**Figure 8.** Comparison of the results of laser scanner outputs with self and pre-calibration dense clouds and RMS errors/standard deviations histograms.

**Table 3.** Comparison results using self and pre-calibration methods.

Calibration methods	RMS error (mm)	Standard deviation ( $\pm$ mm)	Compared results between self-calibration and pre-calibration (%)
Self-calibration (Agisoft)	7.43	5.37	-
Pre-calibration (Agisoft)	7.42	5.44	+0.13
Pre-calibration (MATLAB)	<b>7.21</b>	<b>5.35</b>	<b>+2.96</b>

The project is aiming to take advantage of novel recent technological advancements in computer vision and image-matching along with the “democratization” of the photogrammetric procedure, and also aspires to become a reference research program for future documentations of ecclesiastical heritage of the island of Cyprus, providing high accuracy 3D-textured models and geometrically faithful models and plans to stakeholders and engineers. For this reason, this study aimed and continue to pursue to present in detail the overall procedure starting from the calibration process, to documentation measurements and then to the digital reconstruction, providing in all steps, the details regarding the accuracy level and the difficulties observed during the documentation. The calibration procedure, presented in this study, regards the CANON EOS M5 camera and its application to an ecclesiastical monument of the Bishopric of Cyprus. The final results of this paper indicate that the calibration’s parameters of the digital camera used for

documentation purposes are essential and thus this process will be systematically implemented through the lifetime of the project. Future work can include the validation of other techniques with various types of equipment to further evaluate the extracted 3D metric information. The procedures of the camera’s calibration and the methodologies used will be recorded to provide information about processes of optimization or even to accelerate the procedures of digital documentation of monuments without affecting the desired accuracy or completeness.

### Acknowledgments

This research is supported by the project entitled: “Ecclesiastical Cultural Heritage Digitization Pilots for the Churches of Cyprus and Crete” referred to as “Digital Aposphragisma (Imprint) of Hagionymous Islands” and is co-funded by the European Regional Development Fund (ERDF) and by national funds of Greece and Cyprus, under the Cooperation Programme “INTERREG V-A

Greece-Cyprus 2014-2020". The title/Acronym of the project in the Greek language is: "Πλοηγοί Ψηφιοποίησης Πολιτιστικής Κληρονομιάς Εκκλησιών Κύπρου και Κρήτης"/"Ψηφιακό Αποσφράγισμα Αγιωνύμων νήσων".

## Disclosure statement

No potential conflict of interest was reported by the authors.

## ORCID

Evagoras Evagorou  <http://orcid.org/0000-0001-9441-3946>

## References

- Abed, F. M., Mohammed, M. U., Mohammed, M. U., & Kadhim, S. J. (2019). Architectural and cultural heritage conservation using low-cost cameras. *Applied Research Journal*, 3(12), 376–384. [online] Accessed May 28, 2019, from. <http://arjournal.org>
- Aicardi, I., Chiabrand, F., Maria Lingua, A., & Noardo, F. (2018). Recent trends in cultural heritage 3D survey: The photogrammetric computer vision approach. *Journal of Cultural Heritage*, 32, 257–266. <https://doi.org/10.1016/j.culher.2017.11.006>
- Bolognesi, M., Furini, A., Russo, V., Pellegrinelli, A., & Russo, P. (2015). Testing the low-cost rps potential in 3D cultural heritage reconstruction. *ISPRS - International Archives of the Photogrammetry, Remote Sensing and Spatial Information Sciences*, 40(5W4), 229–235. <https://doi.org/10.5194/isprsarchives-XL-5-W4-229-2015>
- Brutto, M. L., & Dardanelli, G. (2017). Vision metrology and structure from motion for archaeological heritage 3D reconstruction: A case study of various Roman mosaics. *Acta IMEKO*, 6(3), 35–44. [https://doi.org/10.21014/acta\\_imeko.v6i3.458](https://doi.org/10.21014/acta_imeko.v6i3.458)
- Caradonna, G., Tarantino, E., Scaioni, M., & Figorito, B. (2018). Multi-image 3D reconstruction: A photogrammetric and structure from motion comparative analysis. In: Gervasi, O., et al. (eds.) ICCSA 2018, Part V. LNCS, vol. 10964, pp. 305–316. Springer, Cham (2018). [https://doi.org/10.1007/978-3-319-95174-4\\_25](https://doi.org/10.1007/978-3-319-95174-4_25)
- De Reu, J., Plets, G., Verhoeven, G., De Smedt, P., Bats, M., Cherretté, B., De Maeyer, W., Deconynck, J., Herremans, D., Laloo, P., Van Meirvenne, M., & De Clercq, W. (2013). Towards a three-dimensional cost-effective registration of the archaeological heritage. *Journal of Archaeological Science*, 40(2), 1108–1121. <https://doi.org/10.1016/j.jas.2012.08.040>
- Dhonju, H. K., Xiao, W., Sarhosis, V., Mills, J. P., Wilkinson, S., Wang, Z., Thapa, L., & Panday, U. S. (2017). Feasibility study of low-cost image-based heritage documentation in Nepal. *ISPRS - International Archives of the Photogrammetry, Remote Sensing and Spatial Information Sciences*, XLII2(2/W3), 237–242. <https://doi.org/10.5194/isprs-archives-XLII-2-W3-237-2017>
- Faugeras, O. D., Luong, Q.-T., & Maybank, S. J. (1992). *Camera self-calibration: Theory and experiments*. Springer.
- Fiala, M., & Shu, C. (2008). Self-identifying patterns for plane-based camera calibration. *Machine Vision and Applications*, 19(4), 209–216. <https://doi.org/10.1007/s00138-007-0093-z>
- Fraser, C. S. (1997). Digital camera self-calibration. *ISPRS Journal of Photogrammetry and Remote Sensing*, 52(4), 149–159. [https://doi.org/10.1016/S0924-2716\(97\)00005-1](https://doi.org/10.1016/S0924-2716(97)00005-1)
- Fraser, C. S., & Al-Ajlouni, S. (2006). Zoom-dependent camera calibration in digital close-range photogrammetry. *Photogrammetric Engineering & Remote Sensing*, 72(9), 1017–1026. <https://doi.org/10.14358/PERS.72.9.1017>
- Fryskowska, A., Grochala, A., Fryskowska, A., Kedzierski, M., Grochala, A., & Braula, A. (2016). Calibration of low cost RGB and NIR UAV cameras. *Int. Arch. Photogramm. Remote Sens. Spatial Inf. Sci.*, XLI(B1), 817–821, 2016 <https://doi.org/10.5194/isprsarchives-XLI-B1-817-2016>
- Heikkila, J., & Silven, O. (1997). Four-step camera calibration procedure with implicit image correction. *Proceedings of the IEEE Computer Society Conference on Computer Vision and Pattern Recognition*, pp. 1106–1112, IEEE.
- Holy metropolis of limassol: pilgrim's guide - holy metropolis of limassol. (2016). edited by Holy Metropolis of Limassol..
- Koutsoudis, A., Vidmar, B., Ioannakis, G., Arnaoutoglou, F., Pavlidis, G., & Chamzas, C. (2014). Multi-image 3D reconstruction data evaluation. *Journal of Cultural Heritage*, 15(1), 73–79. <https://doi.org/10.1016/j.culher.2012.12.003>
- Marčiš, M. (2014). Quality of 3D Models Generated by SFM Technology. *The Slovak Journal of Civil Engineering*, 21(4), 13–24. <https://doi.org/10.2478/sjce-2013-0017>
- Murtiyoso, A., Grussenmeyer, P., & Freville, T. (2017). Close range UAV accurate recording and modeling of St-Pierre-le-Jeune neo-Romanesque church in Strasbourg (France). *ISPRS - International Archives of the Photogrammetry, Remote Sensing and Spatial Information Sciences*, XLII2(W3), 519–526. <https://doi.org/10.5194/isprs-archives-XLII-2-W3-519-2017>
- Pierdicca, R., Frontoni, E., Malinverni, E. S., Colosi, F., & Orazi, R. (2016). Virtual reconstruction of archaeological heritage using a combination of photogrammetric techniques: Huaca Arco Iris. *Chan Chan, Peru, Digital Applications in Archaeology and Cultural Heritage*, 3(3), 80–90. <https://doi.org/10.1016/J.DAACH.2016.06.002>
- Pollefeys, M., Koch, R., & Gool, L. (1999). Van: Self-calibration and metric reconstruction inspite of varying and unknown intrinsic camera parameters. *International Journal of Computer Vision*, 32(1), 7–25. <https://doi.org/10.1023/A:1008109111715>
- Remondino, F., & Rizzi, A. (2010). Reality-based 3D documentation of natural and cultural heritage sites—techniques, problems, and examples. *Applied Geomatics*, 2(3), 85–100. <https://doi.org/10.1007/s12518-010-0025-x>
- Roncella, R., Re, C., & Forlani, G. (2011). Performance evaluation of a structure and motion strategy in architecture and cultural heritage. *ISPRS - Int. Arch. Photogramm. Remote Sens. Spat. Inf. Sci.*, 38(5), 285–292, doi:10.5194/isprsarchives-xxxviii-5-w16-285-2011, 2012.
- Schad, D. J., & Engbert, R. (2012). The zoom lens of attention: Simulating shuffled versus normal text reading using the SWIFT model. *Visual Cognition*, 20(4–5), 391–421. <https://doi.org/10.1080/13506285.2012.670143>
- Schönberger, J. L., & Frahm, J.-M. (2016). *Structure-from-motion revisited*. [online]. Accessed February 25 2020, from. <https://github.com/colmap/colmap>
- Strecha, C., Zoller, R., Rutishauser, S., Brot, B., Schneider-Zapp, K., Chovancova, V., Krull, M., & Glassey, L. (2014). *Terrestrial 3D mapping using fisheye and perspective sensors*. Pix4D, Available online: [https://www.researchgate.net/publication/272090366\\_](https://www.researchgate.net/publication/272090366_)

- Sturm, P. F., & Maybank, S. J. (1999). On plane-based camera calibration: A general algorithm, singularities, applications. *Proceedings of the IEEE Computer Society Conference on Computer Vision and Pattern Recognition*, 1, 432–437. <https://doi.org/10.1109/cvpr.1999.786974>
- Tang, R., & Fritsch, D. (2013). Correlation Analysis of Camera Self-Calibration in Close Range Photogrammetry. *The Photogrammetric Record*, 28(141), 86–95. <https://doi.org/10.1111/phor.12009>
- Tang, R., Fritsch, D., Cramer, M., & Schneider, W. (2012). A flexible mathematical method for camera calibration in digital aerial photogrammetry. *Photogramm. Eng. Remote Sensing*, 78(10), 1069–1077, doi:10.14358/PERS.78.10.1069, 2012
- Themistocleous, K. (2017). *The use of UAVs to monitor archeological sites: The case study of choirokoitia within the PROTHEGO project*. Proc. SPIE 10444, Fifth International Conference on Remote Sensing and Geoinformation of the Environment (RSCy2017), 104441I, <https://doi.org/10.1117/12.2292351>
- Themistocleous, K., Ioannides, M., Georgiou, S., & Athanasiou, V. (2018). The first attend for a holistic HBIM documentation of UNESCO WHL monument: The case study of Asinou Church in Cyprus.
- Themistocleous, K., Mettas, C., Evagorou, E., & Hadjimitsis, D. G. (2019). *The use of UAVs and photogrammetry for the documentation of cultural heritage monuments: The case study of the churches in Cyprus*. SPIE-Intl Soc Optical Eng.
- Tucci, G., Bonora, V., Conti, A., & Fiorini, L. (2017). *Digital workflow for the acquisition and elaboration of 3D data in a monumental complex: The fortress of Saint John the Baptist in Florence*. ISPRS - Int. Arch. Photogramm. Remote Sens. Spat. Inf. Sci., XLII(2/W5), 679–686, <https://doi.org/10.5194/isprs-archives-XLII-2-W5-679-2017>
- Verhoeven, G. (2011). Taking computer vision aloft - archaeological three-dimensional reconstructions from aerial photographs with photoscan. *Archaeological Prospection*, 18(1), 67–73. <https://doi.org/10.1002/arp.399>
- Westoby, M. J., Brasington, J., Glasser, N. F., Hambrey, M. J., & Reynolds, J. M. (2012). ‘Structure-from-Motion’ photogrammetry: A low-cost, effective tool for geoscience applications. *Geomorphology*, 179, 300–314. <https://doi.org/10.1016/j.geomorph.2012.08.021>
- Zacharek, M., Delis, P., Kedzierski, M., & Fryskowska, A. (2017). Generating accurate 3D models of architectural heritage structures using low-cost camera & open source algorithms. *ISPRS - International Archives of the Photogrammetry, Remote Sensing and Spatial Information Sciences*, 42(5W1), 99–103. <https://doi.org/10.5194/isprs-Archives-XLII-5-W1-99-2017>
- Zhang, Z. (2000). A flexible new technique for camera calibration. *IEEE Transactions on Pattern Analysis and Machine Intelligence*, 22(11), 1330–1334. <https://doi.org/10.1109/34.888718>
- Zhang, Z., Matsushita, Y., & Ma, Y. (2011). Camera calibration with lens distortion from low-rank textures. *Proceedings of the IEEE Computer Society Conference on Computer Vision and Pattern Recognition*, pp. 2321–2328, IEEE Computer Society.